Atomic interface between microwave and optical photons

M. Hafezi,[1,][*] Z. Kim,[1] S. L. Rolston,[1] L. A. Orozco,[1] B. L. Lev,[2] and J. M. Taylor[1]

[1]*Joint Quantum Institute, University of Maryland/National Institute of Standards and Technology, College Park, Maryland 20742, USA*
[2]*Departments of Applied Physics and Physics, and E. L. Ginzton Laboratory, Stanford University, Stanford, California 94305, USA*

A complete physical approach to quantum information requires a robust interface among flying qubits, long-lifetime memory, and computational qubits. Here we present a unified interface for microwave and optical photons, potentially connecting engineerable quantum devices such as superconducting qubits at long distances through optical photons. Our approach uses an ultracold ensemble of atoms for two purposes: quantum memory and to transduce excitations between the two frequency domains. Using coherent control techniques, we examine an approach for converting and storing quantum information between microwave photons in superconducting resonators, ensembles of ultracold atoms, and optical photons, as well as a method for transferring information between two resonators.

PACS number(s): 03.67.Lx, 37.10.Gh, 42.50.Ct, 85.25.−j

Controlling the interaction between quantum bits and electromagnetic fields is a fundamental challenge underlying quantum information science. Ideally, control allows storage, communication, and manipulation of the information at the level of single quanta. Unfortunately, no single degree of freedom satisfies all these criteria simultaneously [1]. Instead, a hybrid approach may take advantage of each system's most attractive properties. For example, optical photons provide a robust long-distance quantum bus [2], while microwave (MW) photons can be easily manipulated using superconducting qubits [3], and atoms can store quantum information for seconds or even minutes [4,5]. We propose an interface between optical, microwave photons, and atomic excitations that takes advantage of each of these properties.

Previous proposals for interfaces of this nature considered magnetic coupling between ultracold atoms [6] or spins [7–11] to superconducting waveguides, or using optomechanics for frequency conversion between optical and MW photons, without providing a medium for storage [12–14]. In a recent proposal, the possibility of coupling ultracold atoms to a nanofiber in the vicinity of a superconducting waveguide or resonator was suggested [Fig. 1(a)] [15]. The evanescent tail of the two-color laser field propagating in the fiber provides the necessary potential to trap atoms close to the nanofiber in the form of a one-dimensional (1D) lattice, which has recently been demonstrated in Ref. [16]. Exponential decay of the optical trapping field allows the atoms to be held close to the superconducting waveguide, leading to a large atom-photon coupling in the microwave domain. Furthermore, the nanofiber provides an optical waveguide both for trap light and for optical access to atoms. Such a system would provide a simultaneous interface between optical and MW photons and atomic ensemble quantum memory.

In this Rapid Communication, we theoretically illustrate how this proposed system enables storage, retrieval, and conversion for optical and MW photons. Experiments have established [17–20] that coherent control techniques of multi-level atoms [4,5], based on electric-dipole coupling in a Λ

system, allow for efficient storage and retrieval of optical photons into atomic excitations from an ensemble of atoms. We adapt this approach to also store and retrieve MW photons. We investigate the effect of finite bandwidth of MW photons on the storage-retrieval process and also the effect of periodicity of the atomic ensemble which can change the propagation of optical photons due to Bragg scattering. We conclude by discussing quantum communication and measurement protocols enabled by our interface as well as the use of nonalkali atoms for enhanced coupling [21].

The storage of photons (either in the MW or optical domain) in atomic excitations in a generic Λ system forms the basis for our interface, and is shown in Fig. 1. Specifically, we start with an optically pumped ensemble of N atoms in one of the hyperfine ground states, $|a\rangle$. A classical control field $\Omega_M(t)$ [or $\Omega_o(t)$] is used to coherently manipulate the coupling between an intermediate state $|b\rangle$ (or $|d\rangle$) and a final ground state $|c\rangle$. These control fields in turn determine the propagation of the quantum field $\hat{\mathcal{E}}_M(t)$ [or $\hat{\mathcal{E}}_o(t)$] coupling $|a\rangle$ to $|b\rangle$ ($|d\rangle$), leading to electromagnetically induced transparency (EIT) and slow light. The evolution of such coupled system is best described by a bosonic dark state polariton [22], with creation operator

$$\hat{\Psi}_i^\dagger(z,t) = \frac{\Omega_i(t)\hat{\mathcal{E}}_i^\dagger(z,t) - g_i\sqrt{N}\hat{S}^\dagger(z,t)}{\sqrt{\Omega_i^2(t) + g_i^2 N}}, \qquad (1)$$

where i corresponds to either optical (O) or MW domains (M). $\hat{S}^\dagger(z,t)$ is the spin-wave creation operator associated with the atomic ground-state coherence $|c\rangle\langle a|$, in the continuum limit [22,23]—we discuss the effect of lattice later in this Rapid Communication. Here g_o (g_M) is the electric (magnetic) dipole coupling between the atoms and the optical (microwave) waveguide photons, respectively, and N is the total number of atoms.

During the entire operation, quantum excitations remain in the form of a dark polariton and the ratio between the enhanced atom-photon coupling and the control field ($\eta_i = g_i\sqrt{N}/\Omega_i$) dictates the mixture between atomic and photonic parts. In particular, when the control is strong ($\eta_i \ll 1$), the polariton is mostly photonic and the system is transparent, with a group velocity near to the speed of light. In contrast, when the control
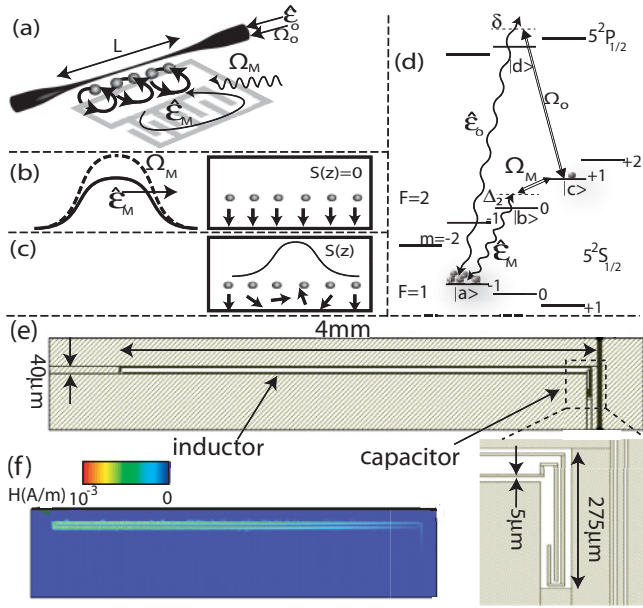
[*]hafezi@umd.edu

FIG. 1. (Color online) (a) Schematics of the interface: Atoms (sphere), in a 1D lattice of the length L, are electrically (magnetically) coupled to light in the nanofiber (the superconducting waveguide), respectively. The quantum microwave (optical) field with Rabi frequency $\hat{\mathcal{E}}_M$ ($\hat{\mathcal{E}}_o$) is manipulated using a classical control radio-frequency (optical) field with Rabi frequency Ω_M (Ω_o), respectively. Trapping lights are not shown in the figure. (b) The quantum ($\hat{\mathcal{E}}_M$) and control (Ω_M) electromagnetic fields arrive while the atomic system is in the ground state. (c) The quantum field is stored as an atomic spin excitation [$S(z)$]. (d) Internal level structure of a ^{87}Rb atom and transitions induced by the four electromagnetic fields. δ,Δ_2 are two-photon and one-photon detunings, respectively. (e) Dimensions of an example LC resonator. (f) Magnetic field profile viewed from the top; lighter colors show higher fields.

is weak ($\eta_i \gg 1$), the polariton is mostly atomic, with a group velocity approaching zero (slow light). Changing the control field allows one to transform a photonic excitation into an atomic excitation and vice versa (see Refs. [4,5]): Once the incoming pulse is entirely inside the system, the control field is adiabatically turned off [$\Omega_i(t) \to 0$], and the excitation will be stored as atomic spin excitations in the ground-state manifold [$S^\dagger(z,t)$] [Figs. 1(b) and 1(c)]. By reversing the control field(s) in time, the stored atomic excitations can later be retrieved as MW or optical photons.

We first address the practical challenges for storing and retrieving MW photons. As an example case, we consider trapped ^{87}Rb atoms coupled to the MW waveguide through the magnetic-dipole interaction, which is characterized by single-photon Rabi frequency g_M [6,15]. The optimal states to preserve the ground-state coherence are the clock states [24,25]: $|a\rangle = |F = 1,m_f = -1\rangle$ and $|c\rangle = |F = 2,m_f = +1\rangle$, as shown in Fig. 1(d). The ground-state decoherence rate is dominated by off-resonant scattering of photons from the trapping lasers which is relatively small, $\gamma \simeq 20$ s^{-1} [16]. The quantum field ($\hat{\mathcal{E}}_M$) and the classical radio-frequency control field (Ω_M) are shown in Fig. 1(d). In order to isolate a single atomic transition to interact with the MW photon, we can use polarization and frequency selectivity. Furthermore, the

application of a moderate magnetic field ($\simeq 6$ mT), leads to a necessary quadratic Zeeman shift and makes the multilevel corrections negligible. For example, as shown in Fig. 1(d), a Zeeman field can split the degeneracy within the hyperfine states so that only the two-photon transition between $|a\rangle$ and $|c\rangle$ is possible.

We review the conditions under which the standard optical EIT storage technique is efficient [4,5,23] and apply them to the microwave domain. We focus on the free-space case, and the generalization to the resonator case can be done by replacement: $c/L \to \kappa$, the resonator decay rate. The bandwidth of the incoming (or retrieval) photon cannot be arbitrarily large. Analytical and numerical calculations have shown that an adiabatic condition must be fulfilled [23], and photons with large bandwidth cannot be stored since the system does not have a fast enough response time. This condition can be intuitively derived, as discussed in Ref. [23]. Briefly, a single spin-wave excitation transfers into the waveguide with a rate $\frac{g_M^2 N}{c/L}$ and decays via a decoherence rate γ. Consequently, via time-reversal symmetry, the bandwidth of an incoming photon to be stored must satisfy $T_p^{-1} \leqslant \frac{g_M^2 N}{c/L}$, where T_p is the pulse duration. The retrieval efficiency is equal to the ratio between the transfer rate and the combined transfer and decay rates, i.e., $1 - \frac{\gamma c/L}{g_M^2 N}$. In the optical domain, this efficiency is simply given by the optical depth of the system, i.e., $\simeq 1 - \frac{\Gamma_{tot} c/L}{4\pi g_o^2 N}$ [23], where Γ_{tot} is the total spontaneous emission rate of the optical transition and where g_o is the single-photon electric-dipole coupling to the fiber.

For a given pulse duration, which satisfies the maximum bandwidth condition (above), the medium should initially be transparent to the pulse ($T_p^{-1} \ll \Delta\omega_{EIT}$), where $\Delta\omega_{EIT}$ is the width of the transparency window. At the same time, the entire pulse should fit inside the medium: $T_p v_g \precsim L$. Given that the group velocity $v_g/c = 1/(1 + \eta_M^2) \simeq \Omega_M^2/g_M^2 N$ and $\Delta\omega_{EIT} \simeq \frac{\Omega_M^2}{\gamma}\sqrt{\frac{\gamma c/L}{g_M^2 N}}$, the last two conditions can only be satisfied in the high cooperativity limit $\frac{g_M^2 N}{\gamma c/L} \gg 1$. In the optical EIT schemes, where the transition decay is dominated by radiative decay, the condition is equivalent to requiring large optical depth. Moreover, the required control field is optimal when the bandwidth of the incoming photon matches the reduced resonator linewidth (due to a slow light effect) [23], i.e., $T_p^{-1} \simeq \frac{\Omega_M^2 \kappa}{g_M^2 N}$.

The bandwidth of MW photons originating in the resonator is given by the resonator bandwidth ($T_p^{-1} \simeq \kappa$). We consider a LC resonator, schematically shown in the Fig. 1(a), where the inductor part is long enough ($\simeq 4$ mm) to accommodate many atoms ($N = 8000$). Using simulation software, we tune the capacitor to achieve a resonance with ^{87}Rb around $\omega_{MW}/2\pi = 6.8$ GHz (for details see Ref. [15]). The magnetic field is relatively uniform along the inductor part, as shown in Fig. 1(f). The corresponding single-photon magnetic coupling is estimated numerically to be $g_M/2\pi = 70$ Hz. Assuming a quality factor $Q \simeq 10^6$, $\kappa \simeq 43$ ms^{-1}, the bandwidth condition can be satisfied. Under these conditions, the magnetic cooperativity is $\frac{g_M^2 N}{\gamma\kappa} \simeq 1700$. The required rf control field should be $\Omega_M/2\pi \simeq 6.3$ kHz. The optical coupling is characterized by the ratio between the spontaneous emission into the fiber and
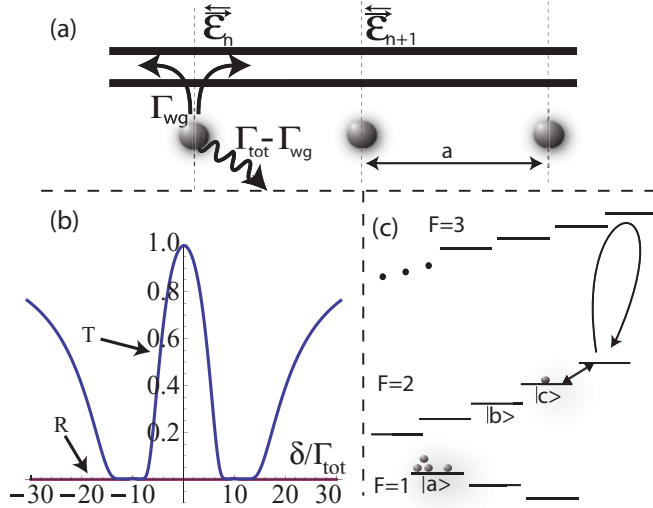
FIG. 2. (Color online) (a) Atoms are periodically coupled to the forward- and backward-going light, in the fiber. (b) The transmission (T) and reflection (R) spectrum of light due to interaction with 1D lattice of atoms. In these plots, $(\Gamma_{wg}, \Omega, c/a)/\Gamma_{tot} = (0.05, 10, 10^7)$, the lattice spacing $a = 500$ nm, and one atom per site is considered. (c) Atomic-level configuration for detecting a single excitation.

the total spontaneous emission, i.e., $\Gamma_{wg}/\Gamma_{tot} = 4\pi g_o^2 L/\Gamma_{tot} c$. This ratio is estimated to be 5% [15]. Therefore, the electrical cooperativity (optical depth) of the system is OD = $N\Gamma_{wg}/\Gamma_{tot} \simeq 400$. The high electric (magnetic) cooperativity guarantees efficient transfer of excitations in the optical (MW) domain, respectively.

We now shift our attention to the unique features of the optical components of our interface. Trapped ^{87}Rb atoms are coupled to light in the optical fiber through the electric-dipole interaction. Since the atoms are trapped in a one-dimensional lattice along the optical fiber, the light propagating inside the fiber experiences periodic scattering in the form of a Bragg grating. The effect of such multiple scatterings can lead to a band-gap structure, in direct analogy to two-level atoms in an optical lattice [26]. Since the atoms are not saturated by small numbers of photons ($\Gamma_{wg}/\Gamma_{tot} \ll 1$), the system is linear, i.e., away from the photon-blockade regime [27,28]. As the atoms are periodically spaced, we can discretize the propagation of the electric field [Fig. 2(a)] and use the transfer-matrix formalism to study these multiple scatterings, due to the three-level transition ($|a\rangle \leftrightarrow |d\rangle \leftrightarrow |c\rangle$) (see the Supplemental Material for details) [29].

The transmission spectrum of a 1D array of 8000 sites ($= L/a$) is shown in Fig. 2(b). We find that our realistic numbers lead to behavior close to that of free space and no band-gap structure is observed [30–32]. In particular, the dips in the transmission spectrum correspond to dressed states split by the Rabi frequency of the control field, in direct analogy to EIT in free space. In the middle of the transparency window, the excitations transform entirely into spin excitation of the atoms. Therefore, once the pulse is inside the atomic medium, by turning off the control field, the photonic excitation can be stored as atomic ground-state excitation. Deviations from this behavior can occur, particularly for stronger single atom-field coupling, but this will be the subject of future research.

In such a hybrid system, we can implement various protocols. First, one can coherently transfer the optical photon, MW photons, and atomic excitation to each other. As mentioned earlier, this process is efficient when the cooperativity is large, $\frac{g_M^2 N}{\gamma c/L} \gg 1$, and the photon pulse duration satisfies $T_p^{-1} \leqslant \frac{g_M^2 N}{c/L}$. This enables a quantum-coherent interconnection between MW excitations and optical photons, which allows for a wide variety of quantum communication and quantum information protocols between distant systems, including quantum repeaters, teleportation-based gates, and distributed quantum computing [33].

Second, in this interface, single photons can be detected with high quantum efficiency. In particular, when the excitation is a photon (either optical or MW), it can transferred to an atomic spin wave. In turn, the atomic spin wave can be transferred to a hyperfine excitation detectable by absorption [34], as shown in Fig. 2(c). More specifically, the single atomic excitation in the form of $|c\rangle\langle a|$ coherence can be efficiently transferred to $|F = 2, m_F = 2\rangle\langle F = 1, m_f = -1|$, using MW and RF control fields [35,36]. Then, using the cycling transition, we can verify the number of original excitations with a high degree of confidence using, e.g., Bayesian inference.

Third, we can generate entanglement between a MW photon and the atomic ensemble in analogy to off-resonant Raman atom-photon entanglement generation [37]. The atomic ensemble should be prepared at the $|c\rangle = |F = 2, m_F = +1\rangle$ level; then applying a rf field coherently generates an anti-Stokes MW photon accompanied with an atomic excitation in the coherence $|F = 2, m_F = +1\rangle\langle F = 1, m_F = -1|$, where the outgoing MW photon and the atomic ensemble are entangled. The efficiency of this process is similar to the storage retrieval of single excitations, as discussed earlier.

Fourth, we can envisage using the hybrid system to induce a large optical nonlinearity via known Josephson junction-based microwave nonlinearities. In particular, when the control fields Ω_o, Ω_M are on, through a four-wave-mixing process, the optical and MW photons will be coupled to each other. Therefore, by adding a nonlinear element for MW photons (e.g., Cooper-pair boxes or superconducting qubits [38,39]), a large optical nonlinearity can be induced for optical photons. Such a large nonlinearity could be harnessed to perform a two-qubit phase gate on optical photons, a key ingredient of deterministic optical quantum computing.

Finally, we can use this system to coherently transfer quantum excitations between two coupled cells, each comprising a resonator and atomic ensemble [Fig. 3(a)] [40–44], where the coupling rate is κ and the intrinsic resonator loss rate is κ_{in}. By changing the control field (Ω_M) in each cell, one can dynamically control the resonator decay rate, i.e., $\kappa/\sqrt{1 + \eta^2}$, and perform dynamical impedance matching [43]. If $\eta_1 \ll 1 \ll \eta_2$, then the dark state in cell one (two) is mostly photonic (atomic), respectively. Therefore, by adiabatically going from $\eta_1 \ll \eta_2$ to $\eta_2 \ll \eta_1$, we can transfer an atomic excitation from cell two to cell one. The process can be performed with high fidelity because the photonic mode is never excited and the system remains in a dark state, as shown in Fig. 3(b), where $\eta_2 = \eta_c^2 \eta_1^{-1}$ and the control field values
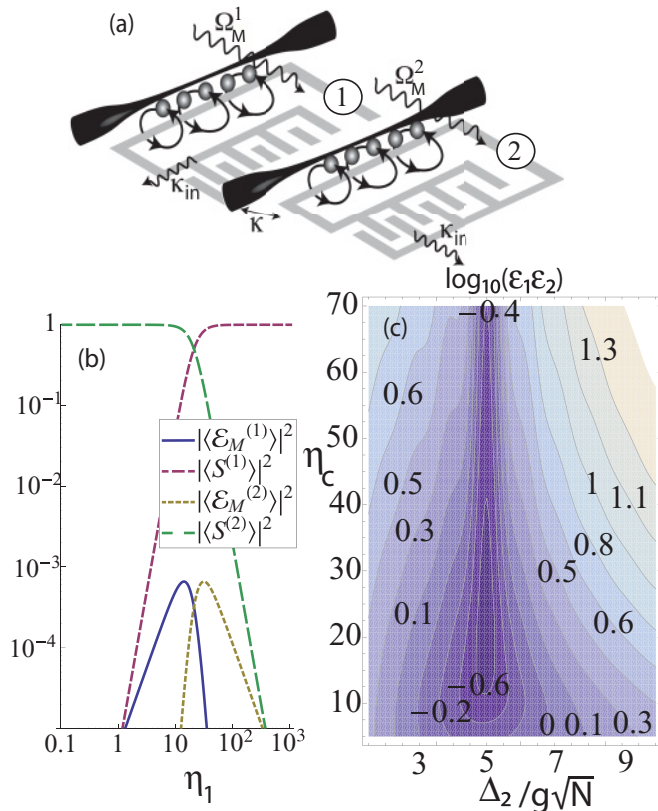
FIG. 3. (Color online) (a) Schematics of two cells (two *LC* resonators are coupled by the rate κ and each having intrinsic loss $\kappa_{\rm in}$), an adiabatic quantum state transfer can be performed, using atomic ensembles. (b) Probabilities of having the excitation in the photonic (normalized $|\langle \mathcal{E}_M^{(1)} \rangle|^2, |\langle \mathcal{E}_M^{(2)} \rangle|^2$) or atomic (normalized $|\langle S^{(1)} \rangle|^2, |\langle S^{(2)} \rangle|^2$) form, as a function of control field η_1, where $\eta_2 = \eta_c^2 \eta_1^{-1}$, for optimized values of $(\eta_c, \Delta_2) \simeq (20, 5)g\sqrt{N}$. (c) The combined adiabaticity-loss condition for crossing value of control fields (η_c) and one-photon detuning (Δ_2), as shown in Fig. 1.

cross at η_c (see the Supplemental Material [29] for details). During this process, two conditions should be satisfied:

(1) adiabaticity, $\sum_{i \neq 4} \frac{|\langle e_4 | \partial_\eta | e_i \rangle|}{e_4 - e_i} \dot{\eta} = \epsilon_1 \dot{\eta} \ll 1$, where $|e_i\rangle$ are energy eigenstates of the system and e_i their corresponding energies, the dark state of interest is $|e_4\rangle$); and (2) negligible loss, $\sum_{i=1,2} \int (\kappa_{\rm in} |\langle \mathcal{E}_M^{(i)} \rangle|^2 + \gamma |\langle S^{(i)} \rangle|^2) \frac{1}{\dot{\eta}} d\eta = \epsilon_2 / \dot{\eta} \ll 1$, where the first (second) term represents the photonic (atomic) loss, respectively. In order to satisfy both, one should have $\epsilon_1 \epsilon_2 \ll 1$ [see Fig. 3(c)]. For relevant experimental parameters $(\kappa, \kappa_{\rm in}, \gamma) \simeq (0.2, 1, 0.0005)g\sqrt{N}$, we find the optimized values for the crossing value of control fields and one-photon detuning to be $(\eta_c, \Delta_2) \simeq (20, 5)g\sqrt{N}$, which makes $\epsilon_1 \epsilon_2 \simeq 0.26$.

We note that implementation of such schemes is within the reach of current technology, although it is challenging. In particular, the long nanofiber (a few cm) should be mounted in the proximity of the superconducting resonator without sagging or breaking [45]. Moreover, the nanofiber polarization and transmission properties should be maintained during the transport into the dilution fridge and the cooling process to millikelvin temperatures. The stray light scattered from the nanofiber can decrease the quality factor of the resonator, and therefore, using a material with higher T_c such as TiN is preferred to Al [46]. While the coupling techniques and protocols proposed here have been presented for alkali atoms, they can be also implemented with rare-earth elements. In particular, for ultracold fermionic Dy [21], one can benefit from $10\times$-enhanced magnetic cooperativity in the rf regime, which, e.g., reduces practical constraints on atom number, while allowing coherent-state transfer to both the telecom regime (1322 nm) and quantum dot transitions (953 nm, 1001 nm). In summary, we have illustrated that an atomic ensemble coupled to an optical and a microwave waveguide can serve as a long-lifetime memory as well as a photon converter between microwave and optical electromagnetic fields.

[1] T. D. Ladd, F. Jelezko, R. Laflamme, Y. Nakamura, C. Monroe, and J. L. O'Brien, Nature (London) **464**, 45 (2010).

[2] J. O'Brien, A. Furusawa, and J. Vučković, Nat. Photonics **3**, 687 (2009).

[3] R. J. Schoelkopf and S. M. Girvin, Nature (London) **451**, 664 (2008).

[4] M. D. Lukin, Rev. Mod. Phys. **75**, 457 (2003).

[5] M. Fleischhauer, A. Imamoglu, and J. Marangos, Rev. Mod. Phys. **77**, 633 (2005).

[6] J. Verdu, H. Zoubi, C. Koller, J. Majer, H. Ritsch, and J. Schmiedmayer, Phys. Rev. Lett. **103**, 043603 (2009).

[7] A. Imamoğlu, Phys. Rev. Lett. **102**, 083602 (2009).

[8] D. Marcos, M. Wubs, J. M. Taylor, R. Aguado, M. D. Lukin, and A. S. Sørensen, Phys. Rev. Lett. **105**, 210501 (2010).

[9] H. Wu *et al.*, Phys. Rev. Lett. **105**, 140503 (2010).

[10] Y. Kubo *et al.*, Phys. Rev. Lett. **105**, 140502 (2010).

[11] R. Amsüss *et al.*, Phys. Rev. Lett. **107**, 060502 (2011).

[12] M. Tsang, Phys. Rev. A **81**, 063837 (2010).

[13] C. Regal, and K. Lehnert, J. Phys.: Conf. Ser. **264**, 012025 (2011).

[14] J. M. Taylor, A. S. Sørensen, C. M. Marcus, and E. S. Polzik, Phys. Rev. Lett. **107**, 273601 (2011).

[15] J. E. Hoffman *et al.*, Rev. Mex. Fis. S **57**, 1 (2011).

[16] E. Vetsch, D. Reitz, G. Sagué, R. Schmidt, S. T. Dawkins, and A. Rauschenbeutel, Phys. Rev. Lett. **104**, 203603 (2010).

[17] B. Julsgaard, J. Sherson, J. I. Cirac, J. Fiurasek, and E. S. Polzik, Nature (London) **432**, 482 (2004).

[18] T. Chaneliere, D. N. Matsukevich, S. D. Jenkins, S. Y. Lan, T. A. B. Kennedy, and A. Kuzmich, Nature (London) **438**, 833 (2005).

[19] M. D. Eisaman, A. Andre, F. Massou, M. Fleischhauer, A. S. Zibrov, and M. D. Lukin, Nature (London) **438**, 837 (2005).

[20] C. W. Chou, H. de Riedmatten, D. Felinto, S. V. Polyakov, S. J. van Enk, and H. J. Kimble, Nature (London) **438**, 828 (2005).

[21] M. Lu, S. H. Youn, and B. L. Lev, Phys. Rev. Lett. **104**, 063001 (2010).

[22] M. Fleischhauer and M. D. Lukin, Phys. Rev. Lett. **84**, 5094 (2000).

[23] A. V. Gorshkov A. Andre, M. Fleischhauer, A. S. Sorensen, and M. D. Lukin, Phys. Rev. Lett. **98**, 123601 (2007); A. V. Gorshkov A. Andre, M. D. Lukin, and A. S. Sorensen, Phys. Rev. A **76**, 033805 (2007); A. V. Gorshkov T. Calarco, M. D. Lukin, and A. S. Sorensen, *ibid*. **77**, 043806 (2008).

[24] P. Treutlein, P. Hommelhoff, T. Steinmetz, T. W. Hänsch, and J. Reichel, Phys. Rev. Lett. **92**, 203005 (2004).

[25] R. Zhao, Y. O. Dudin, S. D. Jenkins, C. J. Campbell, D. N. Matsukevich, T. A. B. Kennedy, and A. Kuzmich, Nat. Phys. **5**, 100 (2008).

[26] I. H. Deutsch, R. J. C. Spreeuw, S. L. Rolston, and W. D. Phillips, Phys. Rev. A **52**, 1394 (1995).

[27] D. E. Chang, A. S. Sørensen, E. A. Demler, and M. D. Lukin, Nat. Phys. **3**, 807 (2007).

[28] J.-T. Shen and S. Fan, Phys. Rev. Lett. **98**, 153003 (2007).

[29] See Supplemental Material at http://link.aps.org/supplemental/ 10.1103/PhysRevA.85.020302 for discussion of dispersive effects of atoms on a 1D lattice such as appearance of a bandgap, and also adiabatic passage between two LC resonators using the dark state.

[30] D. Petrosyan, Phys. Rev. A **76**, 053823 (2007).

[31] J. Nunn *et al.*, Phys. Rev. A **82**, 022327 (2010).

[32] D. Witthaut and A. S. Sørensen, New J. Phys. **12**, 043052 (2010).

[33] D. Bouwmeester *et al.*, *The Physics of Quantum Information* (Springer, New York, 2010).

[34] J. B. Brask, L. Jiang, A. V. Gorshkov, V. Vuletic, A. S. Sørensen, and M. D. Lukin, Phys. Rev. A **81**, 020303 (2010).

[35] S. Chaudhury *et al.*, Phys. Rev. Lett. **99**, 163002 (2007).

[36] S. T. Merkel, P. S. Jessen, and I. H. Deutsch, Phys. Rev. A **78**, 023404 (2008).

[37] L. M. Duan, M. D. Lukin, J. I. Cirac, and P. Zoller, Nature (London) **414**, 413 (2001).

[38] D. Vion, A. Aassime, A. Cottet, P. Joyez, H. Pothier, C. Urbina, D. Esteve, and M. H. Devoret, Science **296**, 886 (2002).

[39] I. Chiorescu, Y. Nakamura, C. Harmans, and J. Mooij, Science **299**, 1869 (2003).

[40] J. I. Cirac, P. Zoller, H. J. Kimble, and H. Mabuchi, Phys. Rev. Lett. **78**, 3221 (1997).

[41] S. J. van Enk, H. J. Kimble, J. I. Cirac, and P. Zoller, Phys. Rev. A **59**, 2659 (1999).

[42] T. Pellizzari, Phys. Rev. Lett. **79**, 5242 (1997).

[43] M. D. Lukin, S. F. Yelin, and M. Fleischhauer, Phys. Rev. Lett. **84**, 4232 (2000).

[44] N. Vitanov, M. Fleischhauer, B. Shore, and K. Bergmann, Adv. At. Mol. Opt. Phys. **46**, 55 (2001).

[45] P. E. Barclay, K. Srinivasan, O. Painter, B. Lev, and H. Mabuchi, Appl. Phys. Lett. **89**, 131108 (2006).

[46] M. Vissers *et al.*, Appl. Phys. Lett. **97**, 232509 (2010).